Utilizing Active Rotor-Current References for Smooth Grid Connection of a DFIG-Based Wind-Power System

Muhammad Arif Sharafat ALI
Department of Electrical and Computer Engineering,
Sungkyunkwan University, Natural Sciences Campus, Suwon 440-746, Republic of Korea
sharafat@skku.edu

***Abstract*—Large inrush currents emerge abruptly whenever a doubly fed induction generator (DFIG) attempts to connect with the grid. Moreover, a DFIG is highly vulnerable to grid disturbances owing to its direct stator-grid contact, which induces a sizable electromotive force in its rotor circuit. Therefore, to ensure reliable and stable system operations, it is unavoidable to improve system performance through suitable and corrective control actions to counteract such issues effectively. In this context, this study focuses on establishing a stable and smooth grid connection for a DFIG by developing dynamic models of the rotor-side converter controls that generate suitable rotor-current references for both the synchronizing and running modes of a DFIG. Furthermore, a smooth transition between both modes is also precisely made with trivial inrush currents. Dynamic simulations confirm the validity of the proposed synchronization method in MATLAB/SIMULINK. Finally, a comparative study with a conventional synchronization method is also performed.**

***Index Terms*—current control, power converters, generators, power grids, wind energy integration.**

I. INTRODUCTION

Wind-power plants (WPPs) are significantly integrated into the existing grid infrastructure to fulfill the desire to shift towards sustainable energy resources. However, this large-scale penetration has opened up new challenges, particularly reducing system stability and security [1–3]. Different countries have amended their grid codes to minimize its adverse impacts to ensure stable and reliable power-system operations [4–5]. Synchronization of a WPP with the grid forms a significant element for convincing a highly safe and quality power system [6]. It implicates synchronizing the voltage amplitude, frequency, and phase angle between the generator and the grid with minimal deviations.

In recent years, doubly fed induction generators (DFIGs) are popular configurations for wind-energy-conversion systems (WECSs) due to their variable-speed operation, high efficiency, and reduced-capacity converters [2]. Inspired by the above background and the upsurge in the permanent magnetic material cost, a DFIG has competitive advantages over the permanent-magnet synchronous generator. Obtaining a direct stator-grid connection, a DFIG is highly susceptible to grid disturbances that persuade a sizable electromotive force in the rotor circuit due to low converter ratings and DC-link voltage limitations. In these situations, both the rotor-side converter (RSC) and the grid-side converter (GSC) are likely to experience overcurrents. In contrast, the DC-link [7–8] undergoes transient overvoltages. Besides, large inrush currents arise whenever a DFIG attempts to establish a connection with the grid.

Despite having extensive literature on the modeling and controls of DFIG-based WECSs [9–12], only a few efforts have been focused on their startup and grid synchronization [6,13–19]. A state-feedback controller for a fast grid connection of a DFIG was developed in [6]. A control scheme for suppressing the stator-current transients during a conventional startup of a DFIG was presented in [13]. The authors of [14] proposed an improved grid synchronization method for a DFIG that controls the positive- and negative-sequence stator voltages to track the grid voltage. A stator flux-oriented vector control to synchronize a DFIG with the grid was employed in [15]. In [16], the authors proposed to start the DFIG as a motor. Afterward, they reversed it to work as a generator. However, this process led to large inrush currents. Detailed analyses of different synchronization methods for renewable energy sources were discussed in [17]. The authors of [18] suggested a synchronization mechanism in which the stator voltage was adjusted equal to the grid voltage by regulating the rotor *d*-axis current. In contrast, the frequency was made to synchronize by rotor-flux angle. The work in [19] proposed a synchronization method based on direct control of stator voltage.

These concerns stated above, need to be addressed to devise a practical method for the smooth integration of WPPs to the grid. The study's ultimate objectives and the proposed technical solutions to achieve them are briefly summarized as follows. Developing an efficient and soft mechanism for grid connection of a DFIG can suppress transient inrush stator and rotor currents effectively to ensure system stability, and it must be capable of reducing electrical stresses on the system in the context of current transients, electromagnetic torque oscillations, and DC-link voltage fluctuations. Moreover, it can also make a smooth transition from synchronizing mode to normal running mode possible. These objectives are achieved by developing different dynamical models for DFIG controls, responsible for operation in both operating modes. Suitable rotor-current references are generated for DFIG controls, which induces stator voltage close to the grid voltage during synchronizing mode. Well-designed proportional-integral (PI) regulators for current controls are embedded in RSC controls for achieving a smooth transition, from synchronizing to normal

Digital Object Identifier 10.4316/AECE.2020.04011

mode, without transients.

In summary, the main contributions of this study are presented as follows:

- A soft synchronization mechanism based on modified DFIG control structures generates the proper rotor-current references for establishing a smooth and stable stator-grid connection with trivial inrush currents, thereby guaranteeing the system stability. Moreover, the electromagnetic torque oscillations and DC-link voltage variations are effectively surpassed.
- Initial errors of rotor position are estimated well and suitably compensated in the DFIG control system during synchronizing mode. Furthermore, the design is efficient and straightforward to implement.
- Simple and effective PI controls are prepared for obtaining a smooth transfer between both operating modes because the change in current references can cause huge transients, thus minimizing the impacts on the DFIG and system operations and maintaining the integrity of the power system operations.

The remainder of this paper is structured as follows: A brief description of a basic wind-driven DFIG system is presented in Section II. In Section III, a mathematical model of a DFIG is reviewed. The basic concepts, detailed formulation, designed procedures, and analyses of the proposed control method are established in Section IV. In Section V, a DFIG system is simulated in MATLAB/SIMULINK, and extensive reviews of the numerical simulations are provided to examine the performance of the proposed control scheme. Further, a comparative study with the conventional synchronization method is also performed. Finally, Section VI presents the concluding remarks.

II. Description of a Grid-Connected DFIG System

Figure 1 presents the basic schematic of the DFIG-based WECS, where the most important components are highlighted. The system comprises a variable-speed WT, a wound-rotor induction generator, RSC, an intermediary DC-link circuit, GSC, a coupling transformer, and an associated control system. As described, the stator is directly connected to the grid via a three-phase transformer and a three-phase stator circuit breaker (SCB); however, the rotor is indirectly integrated through a bidirectional converter.

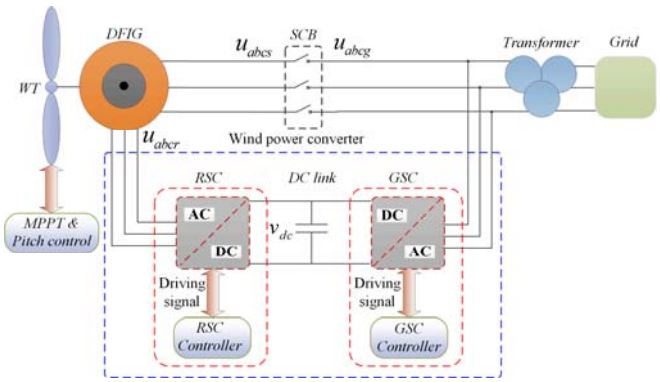

Figure 1. Block diagram of a wind-driven DFIG system

III. DFIG Modeling

The dynamical behavior of a DFIG is analyzed in the synchronous reference frame (SRF) [11, 20], and the voltage and flux equations can be explained as

$$\begin{aligned}
v_{ds} &= R_s i_{ds} + \frac{d\psi_{ds}}{dt} - \omega_s \psi_{qs} \\
v_{qs} &= R_s i_{qs} + \frac{d\psi_{qs}}{dt} + \omega_s \psi_{ds} \\
v_{dr} &= R_r i_{dr} + \frac{d\psi_{dr}}{dt} - \omega_{sl} \psi_{qr} \\
v_{qr} &= R_r i_{qr} + \frac{d\psi_{qr}}{dt} + \omega_{sl} \psi_{dr} \\
\psi_{ds} &= L_s i_{ds} + L_m i_{dr} \\
\psi_{qs} &= L_s i_{qs} + L_m i_{qr} \\
\psi_{dr} &= L_r i_{dr} + L_m i_{ds} \\
\psi_{qr} &= L_r i_{qr} + L_m i_{qs} \\
L_s &= L_{ls} + L_m \\
L_r &= L_{lr} + L_m \\
\omega_{sl} &= \omega_s - \omega_r
\end{aligned} \tag{1}$$

where, v_{ds} and v_{qs} are the stator voltage components in dq-frame; i_{ds} and i_{qs} are the stator current components in dq-frame; Ψ_{ds} and Ψ_{qs} are the stator-flux linkages in dq-frame; R_s and R_r are the stator and rotor winding resistances, respectively; L_s and L_r are the stator and rotor inductances, respectively; L_{ls} and L_{lr} are the stator and rotor leakage inductances, respectively; ω_s is the electrical angular frequency of the SRF; ω_r is the rotor angular frequency; ω_{sl} is the slip angular frequency.

Stator voltage-oriented control (SVOC) is applied to the DFIG model (1) in which the d-axis is associated with the stator voltage. In large-scale WECSs, the generator's stator resistance is generally minimal and can be ignored to simplify the analyses [11]. From (1), the stator currents can be expressed as

$$\left.\begin{aligned} i_{ds} &= \frac{\psi_{ds} - L_m i_{dr}}{L_s} \\ i_{qs} &= \frac{\psi_{qs} - L_m i_{qr}}{L_s} \end{aligned}\right\} \tag{2}$$

Inserting (2) into (1), the rotor fluxes are calculated as

$$\left.\begin{aligned} \psi_{dr} &= \frac{L_m}{L_s}\psi_{ds} + \sigma L_r i_{dr} \\ \psi_{qr} &= \frac{L_m}{L_s}\psi_{qs} + \sigma L_r i_{qr} \end{aligned}\right\}, \quad \sigma = 1 - \frac{L_m^2}{L_s L_r} \tag{3}$$

where, σ denotes the leakage coefficient. Substituting (3) into (1), the rotor voltages are expressed as:

$$\left.\begin{aligned} v_{dr} &= \left(R_r + \sigma L_r \frac{d}{dt}\right) i_{dr} - \omega_{sl}\sigma L_r i_{qr} + \frac{L_m}{L_s}\left(\frac{d\psi_{ds}}{dt} - \omega_{sl}\psi_{qs}\right) \\ v_{qr} &= \left(R_r + \sigma L_r \frac{d}{dt}\right) i_{qr} + \omega_{sl}\sigma L_r i_{dr} + \frac{L_m}{L_s}\left(\frac{d\psi_{qs}}{dt} + \omega_{sl}\psi_{ds}\right) \end{aligned}\right\} \tag{4}$$

The stator-voltage equations in (1) can be simplified further by ignoring the transient terms and are rewritten as

$$\left.\begin{aligned} v_{ds} &\cong -\omega_s \psi_{qs} \\ v_{qs} &\cong \omega_s \psi_{ds} \end{aligned}\right\} \quad (5)$$

By substituting (5) into (4), the rotor voltages can be expressed as

$$\left.\begin{aligned} v_{dr} &= \left(R_r + \sigma L_r \frac{d}{dt}\right) i_{dr} - \omega_{sl} \sigma L_r i_{qr} + \frac{L_m}{L_s}\frac{\omega_{sl}}{\omega_s} v_{ds} \\ v_{qr} &= \left(R_r + \sigma L_r \frac{d}{dt}\right) i_{qr} + \omega_{sl} \sigma L_r i_{dr} + \frac{L_m}{L_s}\frac{\omega_{sl}}{\omega_s} v_{qs} \end{aligned}\right\} \quad (6)$$

The electromagnetic torque (T_{em}) can be calculated as (7) [19]:

$$T_{em} = 1.5p\frac{L_m}{L_s}\left(\psi_{qs} i_{dr} - \psi_{ds} i_{qr}\right) \quad (7)$$

IV. Proposed Grid-Synchronization Mechanism

This section presents the proposed synchronization method for performance improvement of the DFIG by overcoming the problems associated with the rapid onset of the sizable inrush currents. This study is carried out:

- First, some basic concepts of the synchronization are discussed for well-understanding of the entire process.
- Second, the errors related to the initial position of the speed sensor/encoder are estimated.
- Third, the required position angles for obtaining the accurate coordinate transformation are achieved.
- Finally, the designed control structures of the RSC are explained.

A voltage is induced in the stator windings by properly controlling the rotor *dq* currents, whereas the SCB is opened. The induced stator voltage must be equal to grid voltage with minimal deviations regarding the amplitude, frequency, and phase. There are some criteria defined in IEEE1547 for successful implementation of grid synchronization that the system must acquire and these are provided below (see Table I) [21].

Table I. IEEE1547 Synchronization Parameters Limits

Aggregate rating of DR units (kVA)	Frequency difference (Δf, Hz)	Voltage difference (ΔV, %)	Phase angle difference (Δθ, °)
>1500–10,000	0.1	3	10

SVOC is used in the RSC control system that results in relatively independent controls of *d*- and *q*-axis currents. The resultant stator voltages are expressed by

$$\left.\begin{aligned} v_{ds} &\cong V_s \\ v_{qs} &\cong 0 \end{aligned}\right\} \quad (8)$$

Based on (8) and (5), the stator fluxes can be derived as

$$\left.\begin{aligned} \psi_{ds} &\cong 0 \\ \psi_{qs} &\cong -\frac{v_{ds}}{\omega_s} \end{aligned}\right\} \quad (9)$$

Prior information about the initial position of the rotor-speed sensor/encoder must be known. Due to the mechanical coupling of the encoder to the rotor-axis, two types of errors concerning the initial rotor position are needed to be accounted for. The first error is related to the encoder's mounting, and it is necessary to compensate for this error during the synchronization process. The value of this error (θ_{error}) is kept at 30° in this study. The second error is the correct adjustment of the encoder. It arises when the absolute zero-position of the rotor encoder does not coincide with the zero-location of the rotor windings. It should be noticed that the DFIG control performance will worsen if no appropriate remedy is introduced to correct the angle shift between two zeros.

Further, in SVOC of a DFIG, two angles are essential. The first one is the grid-voltage phase angle (θ_s) and is determined by a phase-locked loop (PLL). The second is the rotor-position angle (θ_r), which is obtained by an encoder. These angles must be known to achieve accurate coordinate transformation for rotor currents. As described earlier in this section, v_{qs} is zero in SVOC, and this null value is an indicator of the correct sensor position. The non-zero value of this stator-voltage component should be fed to a PI regulator to obtain the compensation angle ($\theta_{comp.}$). Thus, the resultant rotor-position angle can be calculated as

$$\theta_{comp.} = PI\left(0 - v_{qs}\right) \quad (10)$$

$$\theta_r = p\theta_m - \theta_{error} + \theta_{comp.} \quad (11)$$

Sizable inrush stator and rotor currents occur whenever a stator connection to the grid is made. The proposed control scheme based on generating suitable rotor-current references for both the synchronizing and running modes mitigates inrush currents to ensure a reliable and smooth grid connection. Well-designed PI current regulators are used to achieve a soft mode switching, from synchronizing to running mode. Detailed mathematical modeling, designed approaches, and analyses of RSC controls for each operating mode are explained well in the following subsections.

A. RSC Control Scheme in Synchronizing Mode

The control objective in synchronizing mode is to bring the stator voltage close enough to the grid voltage for making a smooth stator-grid connection possible. Initially, the stator currents of a DFIG are zero (12), as the SCB is opened.

$$\left.\begin{aligned} i_{ds} &= 0 \\ i_{qs} &= 0 \end{aligned}\right\} \quad (12)$$

Inserting stator currents (12) into (1), the stator and rotor fluxes are

$$\left.\begin{aligned} \psi_{ds} &= L_m i_{dr} \\ \psi_{qs} &= L_m i_{qr} \\ \psi_{dr} &= L_r i_{dr} \\ \psi_{qr} &= L_r i_{qr} \end{aligned}\right\} \quad (13)$$

By substituting stator fluxes (13) into (5), the resultant stator *dq* voltages are expressed as

$$\left.\begin{aligned} v_{ds} &\cong -\omega_s L_m i_{qr} \\ v_{qs} &\cong \omega_s L_m i_{dr} \end{aligned}\right\} \quad (14)$$

From (14), it can be concluded that the rotor currents in synchronizing mode regulate the stator voltages. Combining

the last two equations of (13) and the rotor *dq* voltages from (1), the modified expressions for the rotor *dq* voltages are

$$\left.\begin{aligned} v_{dr} &= R_r i_{dr} + L_r \frac{d}{dt} i_{dr} - \omega_{sl} L_r i_{qr} \\ v_{qr} &= R_r i_{qr} + L_r \frac{d}{dt} i_{qr} + \omega_{sl} L_r i_{dr} \end{aligned}\right\} \quad (15)$$

Equation (15) shows that the rotor currents depend on rotor voltage. The dynamical model of a DFIG in synchronizing mode is represented by (14) and (15). Analytical expressions for rotor-current references in synchronizing mode are represented by

$$\left.\begin{aligned} i_{dr-ref} &= 0 \\ i_{qr-ref} &= -\frac{v_{ds}}{\omega_s L_m} + PI\left(|v_s| - |v_g|\right) \end{aligned}\right\} \quad (16)$$

The second term (right-hand side) of $i_{qr\text{-}ref}$ in (16) is the output of a transient-voltage regulator (TVR), which is designed to cater to the effects of the stator overvoltage that arises when the SCB closes. The control diagram of the RSC in synchronizing mode is presented in Fig. 2. Combining the PI outputs of the current-control loops and the decoupling terms ($v_{dr\text{-}comp.}$ and $v_{qr\text{-}comp.}$), the rotor-voltage references are obtained by (17), which are applied to generate the switching signals for RSC.

$$\left.\begin{aligned} v_{dr-ref} &= PI\left(i_{dr-ref} - i_{dr}\right) + v_{dr-comp.} \\ v_{qr-ref} &= PI\left(i_{qr-ref} - i_{qr}\right) + v_{qr-comp.} \\ v_{dr-comp.} &= -\omega_{sl} L_r i_{qr} \\ v_{qr-comp.} &= \omega_{sl} L_r i_{dr} \end{aligned}\right\} \quad (17)$$

B. RSC Control Scheme in Running Mode

After establishing a connection to the grid, the DFIG starts to generate active power through RSC. Using (2) and (9) to derive a direct relation between the stator and rotor currents.

$$\left.\begin{aligned} i_{ds} &= -\frac{L_m}{L_s} i_{dr} \\ i_{qs} &= -\frac{v_{ds}}{\omega_s L_s} - \frac{L_m}{L_s} i_{qr} \end{aligned}\right\} \quad (18)$$

Putting (9) into (7) yields the electrometric torque as

$$T_{em} = -1.5 p \frac{L_m}{\omega_s L_s} v_{ds} i_{dr} \quad (19)$$

The stator active and reactive powers in SVOC are

$$\left.\begin{aligned} P_s &= 1.5\left(v_{ds} i_{ds} + v_{qs} i_{qs}\right) = 1.5 v_{ds} i_{ds} \\ Q_s &= 1.5\left(v_{qs} i_{ds} - v_{ds} i_{qs}\right) = -1.5 v_{ds} i_{qs} \end{aligned}\right\} \quad (20)$$

By substituting (18) into (20), the above expressions can be rewritten as

$$\left.\begin{aligned} P_s &= -1.5 \frac{L_m}{L_s} v_{ds} i_{dr} \\ Q_s &= 1.5 \frac{v_{ds}}{L_s}\left(\frac{v_{ds}}{\omega_s} + L_m i_{qr}\right) \end{aligned}\right\} \quad (21)$$

Equation (3) can be further simplified by putting (9) into it, and the resultant rotor fluxes are written as

$$\left.\begin{aligned} \psi_{dr} &= \sigma L_r i_{dr} \\ \psi_{qr} &= \sigma L_r i_{qr} - \frac{L_m}{\omega_s L_s} v_{ds} \end{aligned}\right\} \quad (22)$$

Inserting (9) into (4), the dynamical model of a DFIG in terms of rotor *dq* voltages can be expressed by

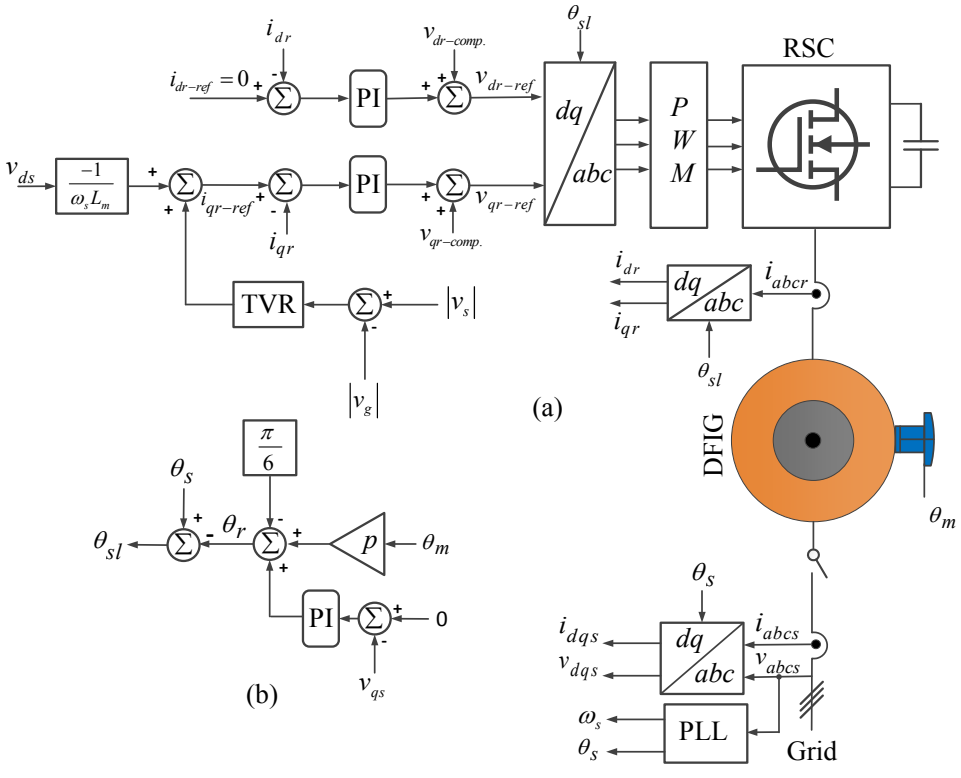

Figure 2. Schematic of the RSC control scheme in synchronizing mode: (a) RSC control and (b) slip-angle calculation

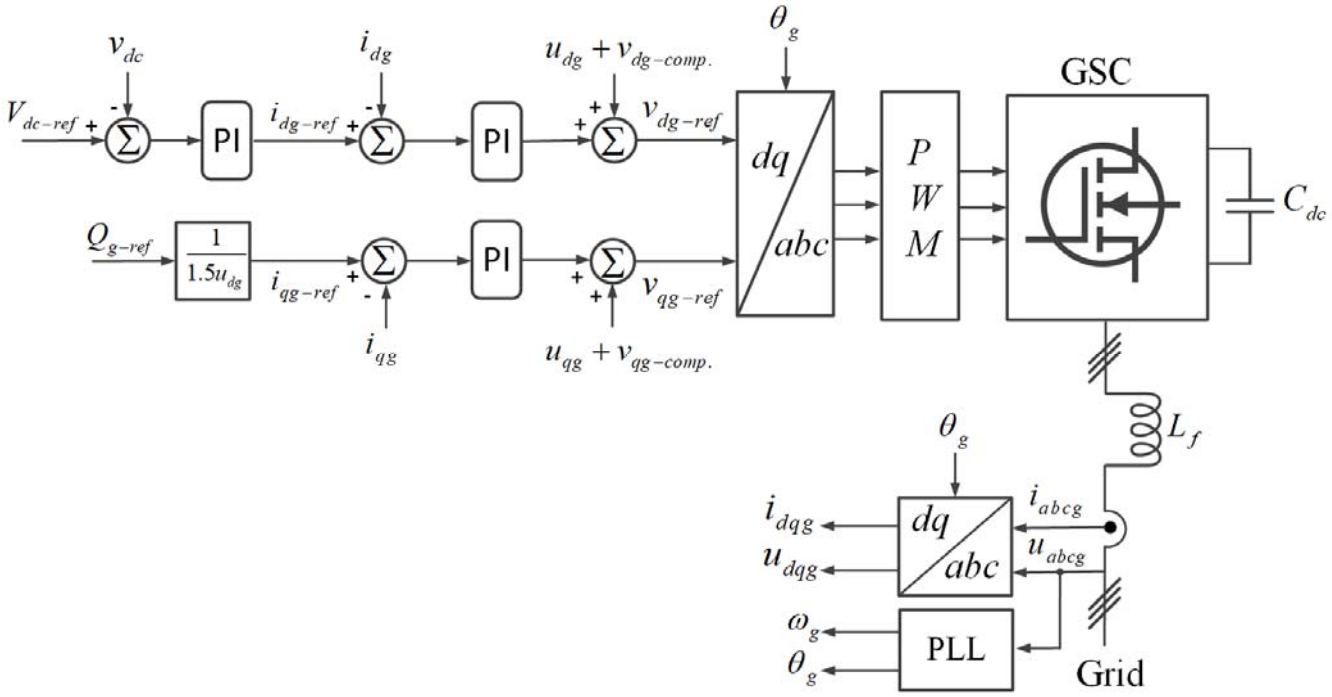

Figure 3. Schematic of the RSC control scheme in running mode

$$\left.\begin{aligned} v_{dr} &= R_r i_{dr} + \sigma L_r \frac{d}{dt} i_{dr} - \omega_{sl}\sigma L_r i_{qr} + \frac{\omega_{sl}}{\omega_s}\frac{L_m}{L_s} v_{ds} \\ v_{qr} &= R_r i_{qr} + \sigma L_r \frac{d}{dt} i_{qr} + \omega_{sl}\sigma L_r i_{dr} \end{aligned}\right\}, v_{qs} = 0 \tag{23}$$

The schematic of the RSC control scheme in the running mode is depicted in Fig. 3. The rotor *d*-axis current reference ($i_{dr\text{-}ref}$) is obtained from torque command (19); however, $i_{qr\text{-}ref}$ is estimated by combining (second equation of (21)) and the TVR output. The rotor-current references are given as

$$\left.\begin{aligned} i_{dr-ref} &= -\frac{\omega_s L_s}{1.5 p L_m v_{ds}} T_{em-ref} \\ i_{qr-ref} &= \frac{L_s}{1.5 L_m v_{ds}} Q_{s-ref} - \frac{v_{ds}}{\omega_s L_m} + PI\left(|v_s| - |v_g|\right) \end{aligned}\right\} \tag{24}$$

Because the rotor provides magnetizing current, the stator reactive-power reference is taken as zero [10]. Here, $T_{em\text{-}ref}$ is the output of the maximum power point tracking controller (MPPT) and is obtained as

$$T_{em-ref} = k_m \omega_r^2 - F\omega_r - D \tag{25}$$

In (25), k_m denotes the maximum power at base wind speed; however, F and D are the coefficients of the losses. Mathematical expressions for rotor-voltage references in running mode are given by

$$\left.\begin{aligned} v_{dr-ref} &= PI\left(i_{dr-ref} - i_{dr}\right) + v_{dr-comp.} + \frac{\omega_{sl} L_m}{\omega_s L_s} v_{ds} \\ v_{qr-ref} &= PI\left(i_{qr-ref} - i_{qr}\right) + v_{qr-comp.} \\ v_{dr-comp.} &= -\sigma\omega_{sl} L_r i_{qr} \\ v_{qr-comp.} &= \sigma\omega_{sl} L_r i_{dr} \end{aligned}\right\} \tag{26}$$

V. Simulation Results and Discussions

This section deals with the suitability and validation of the proposed scheme developed in Section IV for the smooth grid integration of a DFIG. The DFIG parameters are taken from [20] and are provided in Table II. The parameters of PI regulators are referred to in Table III. Simulation studies in MATLAB/SIMULINK are performed to demonstrate the performance of the proposed synchronization scheme. Two cases for different values of the initial slip (s_{ini}) are considered.

Table II. Parameters of 1.5MW DFIG System

Parameter	Value	Unit
Nominal mechanical power	1.5	MW
Nominal stator line-to-line voltage	690	V (rms)
Rated frequency	50	Hz
Rated rotor speed	1750	rpm
Pole pairs	2	Nos.
Rated mechanical torque	8.185	kNm
Stator resistance	2.65	mΩ
Rotor resistance	2.63	mΩ
Stator leakage inductance	0.1687	mH
Rotor leakage inductance	0.1337	mH
Mutual inductance	5.4749	mH
Inertia constant	3	s
DC-link voltage reference	1150	V

Table III. Parameters of PI Controllers

Controller	K_p	K_i
Synchronizing mode		
Current controllers	14.1	6.598
Transient voltage regulator	0.002389	0.3002
Rotor-position compensation controller	0.1	1
Running mode		
Current controllers	0.664	6.599

A. Case 1: Performance of the Proposed Synchronization Scheme (s_{ini} = 0.2)

The validity of the proposed synchronization process is investigated herein. Initially, the stator windings are disconnected from the grid as the SCB is turned off, and the RSC generates the rotor current, i.e., $i_{qr\text{-}ref}$. On the other hand, the rotor *d*-axis current reference ($i_{dr\text{-}ref}$) is maintained at zero. The GSC operates first and develops the DC-link (v_{dc}) up to its rated value. Figures 4(a)–(f) present the simulation results of generator torque, DC-link voltage, rotor current, rotor *d*- and *q*-axis currents, and stator current, respectively. Figure 4(a) illustrates that the generator torque in the synchronizing mode is nearly zero and goes into the generating mode smoothly when the SCB closes. It is evidence of establishing a smooth stator-grid connection.

Figure 4(b) depicts the DC-link voltage maintained at its nominal value, which validates the excellent efficiency of the designed regulators. The insignificant rotor inrush currents, as observed in Fig. 4(c) indicates the strength of the proposed synchronization method. The rotor *dq* currents are appropriately regulated and rigorously follow their reference values, respectively, and are presented by Figs. 4(d)–(e). Figure 4(f) shows a specified portion of the stator current at the instant of SCB closure, proving the suitability of the proposed scheme in mitigating the transient currents. The simulation results reveal that a smooth and stable grid connection of a DFIG is established with trivial stator- and rotor-inrush currents when the proposed scheme is applied.

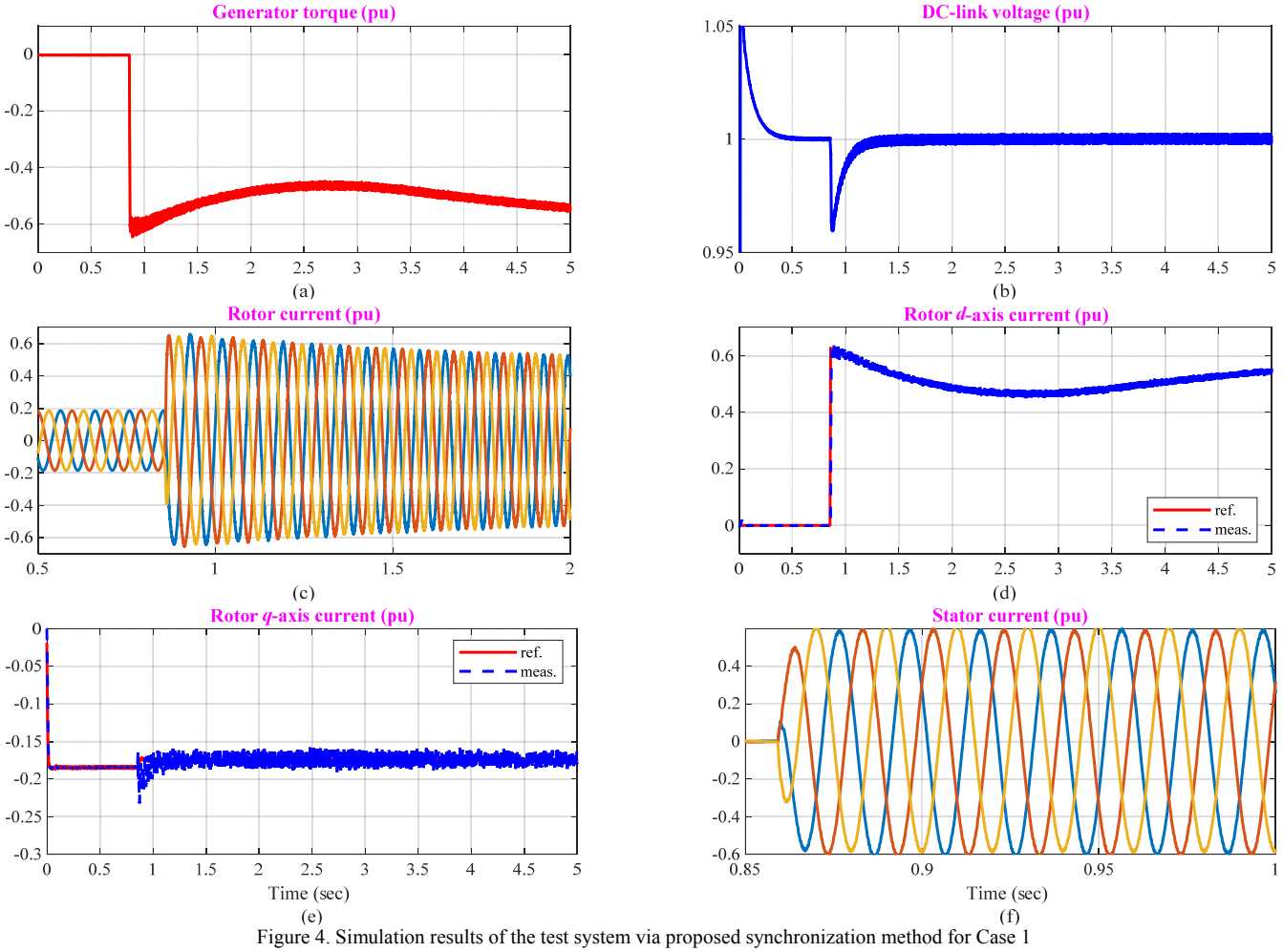

Figure 4. Simulation results of the test system via proposed synchronization method for Case 1

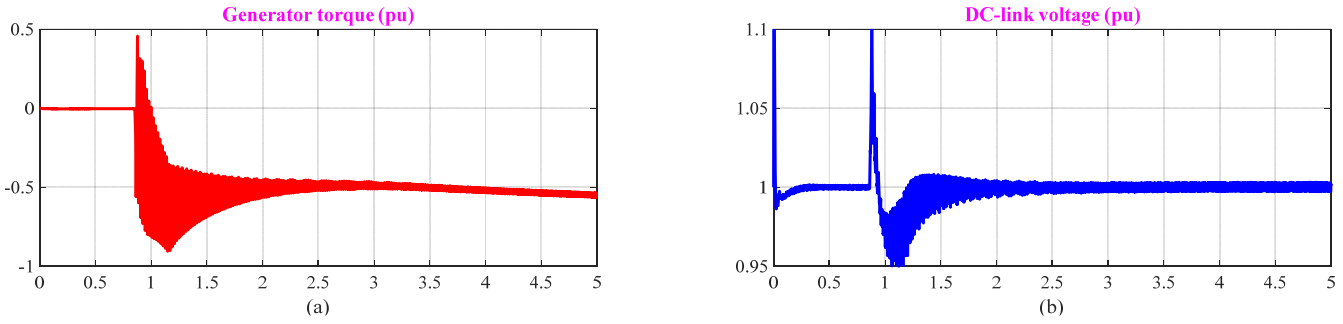

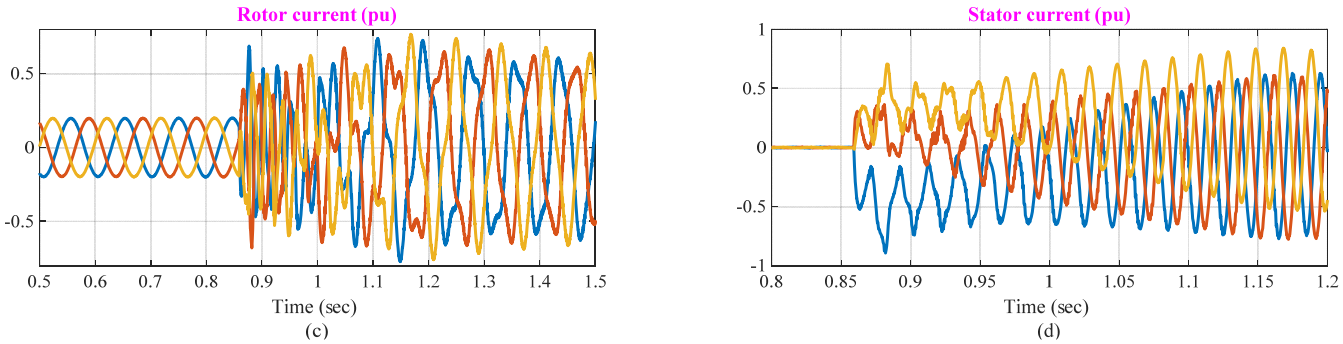

Figure 5. Simulation results of the test system via conventional synchronization method for Case 1

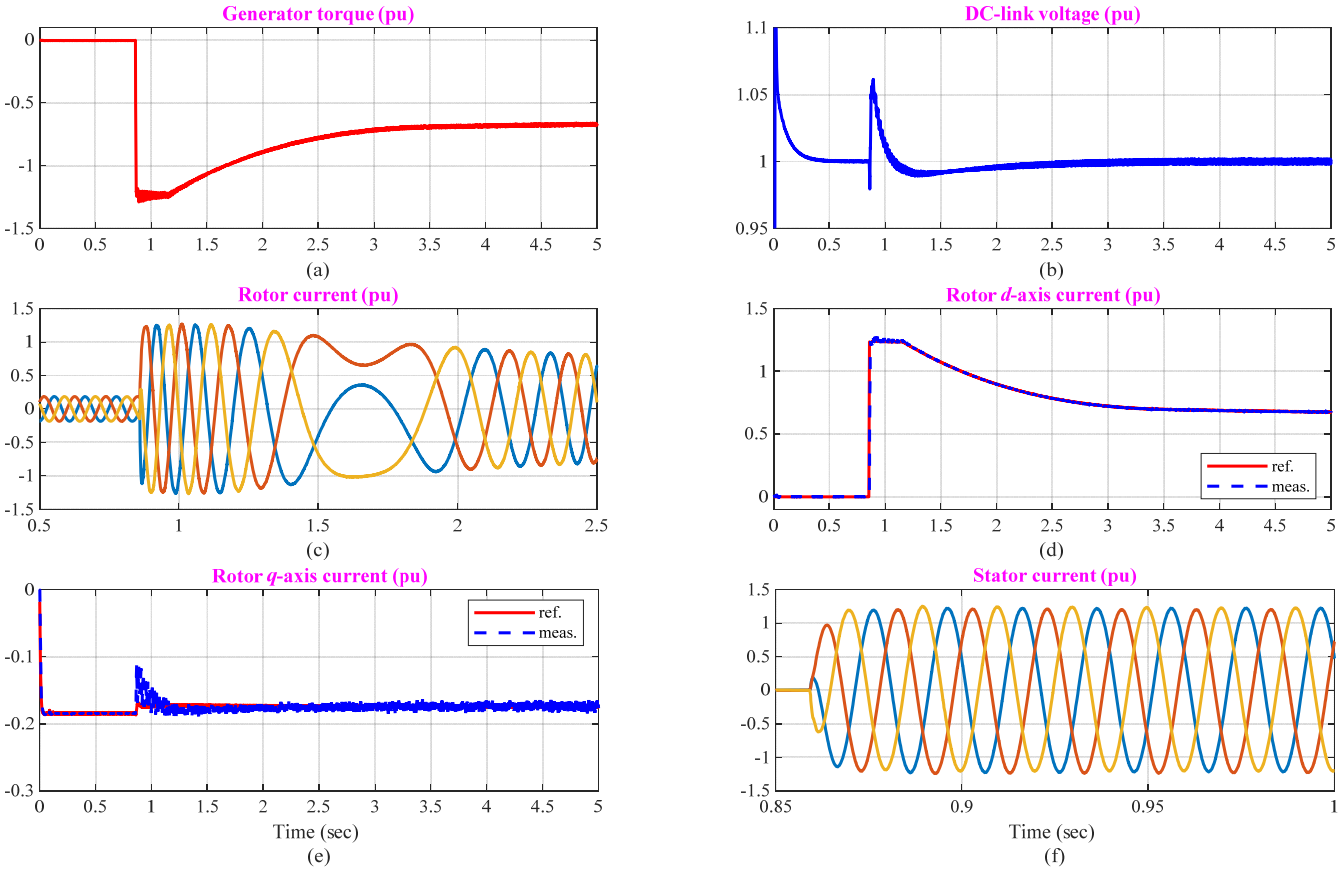

Figure 6. Simulation results of the test system via proposed synchronization method for Case 2

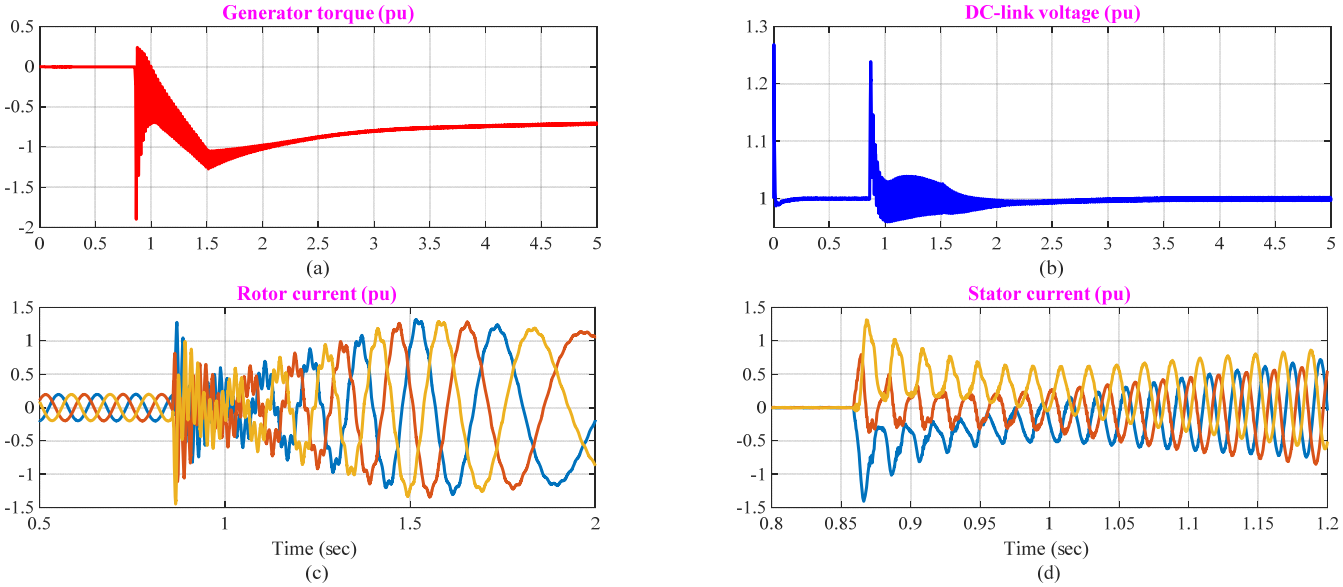

Figure 7. Simulation results of the test system via conventional synchronization method for Case 2

It is of interest to analyze the system performance via the conventional synchronization method for comparison purposes, and the resultant waveforms of the selected quantities are presented in Fig. 5. As can be seen from Fig. 5(a) that the generator torque goes into the motoring mode with huge transients at SCB closure. It can be figured out from Fig. 5(b) that the DC-link voltage variations (more than 10%) are higher compared to the result realized using the proposed scheme (see Fig. 4(b)). The significant stator- and rotor-current transients are also noticed in Figs. 5(c)–(d), which show that the conventional method is less reliable than the established design.

Summarizing, the proposed synchronization method establishes a safe and stable connection of a DFIG with the grid and avoids inrush currents. Moreover, the switching process between both modes is also smooth, which is confirmed from Fig. 4.

B. Case 2: Performance of the Proposed Synchronization Scheme (s_{ini} = -0.2)

The system is simulated again for Case 2, and the simulation results of the selected quantities using proposed and conventional synchronization methods are shown in Figs. 6–7, respectively. As expected, the proposed synchronization method offers a stable stator-grid connection, as shown in Fig. 6, without inrush currents, thereby ensuring system security. On the other hand, significant transients in stator and rotor currents are observed, which can be seen in Fig. 7(c)–(d) when the conventional method is applied. Moreover, massive electromagnetic torque and DC-link voltage variations can be observed in Fig. 7(a)–(b).

Thus, it can be concluded from the simulation results that the proposed method has adequately reflected the superior performance compared with the conventional method in terms of current transients and torque oscillations. Hence, the application of the proposed method is a promising alternative to grid connection and has potential in wind-energy integration.

VI. CONCLUSION

This study addressed a critical issue of grid integration of a DFIG-based WECS that was raised with the significant penetration of wind power into the system and presented a technical solution based on generating appropriate rotor-current references for solving it. This paper can be concluded as follows:

1. A soft and efficient synchronization method for the grid connection of a DFIG-based WECS was presented and validated via simulation results. It revealed its effectiveness in suppressing the transient inrush stator and rotor currents, electromagnetic torque oscillations, and DC-link voltage variations thus play a crucial and critical role in maintaining system stability.
2. It also made a stable and smooth grid connection of a DFIG possible. Moreover, suitable compensation in respect of initial errors of the rotor position was provided.
3. Finally, a control-performance comparison with the conventional synchronization method was provided. Four important system variables namely, stator and rotor currents, electromagnetic torque, and DC-link voltage are considered. Simulation results showed that
   - The proposed method effectively limited transient stator and rotor currents. In contrast, the conventional method produced unsymmetrical and high-frequency inrush transients thus had adverse impacts on DFIG and power converters.
   - Huge electromagnetic-torque oscillations in case of applying the conventional method had put a question mark on system stability. Notably, at the instant of circuit breaker closure, the DFIG behaved as an induction generator and absorbed reactive power from the grid.
   - Acceptable DC-link voltage variations (within 6% of the rated value) were achieved by the proposed method. In contrast, the conventional method generated large voltage fluctuations with a peak of above 15% of its rated value.

REFERENCES

[1] M. A. S. Ali, K. K. Mehmood, C. H. Kim, "Full operational regimes for SPMSG-based WECS using generation of active current references," International Journal of Electrical Power & Energy Systems, vol. 112, pp. 428-441, 2019. doi:10.1016/j.ijepes.2019.05.028

[2] A. Mohammadi, S. Tavakoli, S. M. Barakati, "On power tracking and alleviation by a new controller for fulfilment of the damping and performance requisites for a variable speed wind system: An optimal approach," International Journal of Electrical Power & Energy Systems, vol. 75, pp. 187-193, 2016. doi:10.1016/j.ijepes.2015.07.038

[3] M. A. S. Ali, K. K. Mehmood, S. Baloch, C. H. Kim, "Wind-speed estimation and sensorless control for SPMSG-based WECS using LMI-based SMC," IEEE Access, vol. 8, pp. 26524-26535, 2020. doi:10.1109/ACCESS.2020.2971721

[4] M. A. S. Ali, K. K. Mehmood, C. H. Kim, "Power system stability improvement through the coordination of TCPS-based damping controller and power system stabilizer," Advances in Electrical and Computer Engineering, vol. 17, no. 4, pp. 27-36, 2017. doi:10.4316/AECE.2017.04004

[5] M. A. S. Ali, K. K. Mehmood, J. K. Park, C. H. Kim, "Battery Energy Storage System-Based Stabilizers for Power System Oscillations Damping," Journal of the Korean Institute of Illuminating and Electrical Installation Engineers, vol. 10, pp. 75-84, 2016. doi:10.5207/JIEIE.2016.30.10.075

[6] A. G. Abo-Khalil et al., "Design of state feedback current controller for fast synchronization of DFIG in wind power generation systems," Energies, 12, 2427, 2019. doi:10.3390/en12122427

[7] A. M. A. Haidar, K. M. Muttaqi, M. T. Hagh, "A coordinated control approach for DC link and rotor crowbars to improve fault ride-through of DFIG-based wind turbine," IEEE Transactions on Industry Applications, vol. 53, no. 4, pp. 4073-4086, 2016. doi:10.1109/TIA.2017.2686341

[8] M. A. S. Ali, K. K. Mehmood, J. S. Kim, C. H. Kim, "ESD-based crowbar for mitigating DC-link variations in a DFIG-based WECS," 2019 International Conference on Power Systems Transients (IPST), Perpignan, 2019, pp. 1-6.

[9] Y. Yaramasu, B. Wu, P. C. Sen, S. Kouro, M. Narimani, "High-power wind energy conversion systems: state-of-the-art and emerging technologies," in Proceedings of the IEEE, vol. 103, no. 5, pp. 740-788, 2015. doi:10.1109/JPROC.2014.2378692

[10] G. Abad, J. Lopez, M. Rodriguez, L. Marroyo, G. Iwanski, "Doubly fed induction machine: modeling and control for wind energy generation", Wiley-IEEE, pp. 209-218, 199, 2011

[11] F. Blaabjerg, D. Xu, W. Chen, N. Zhu, "Advanced control of doubly fed induction generator for wind power systems", Wiley-IEEE, pp. 81-85, 116, 2018. doi:10.1002/9781119172093

[12] B. Wu, Y. Lang, N. Zargari, S. Kouro, "Power conversion and control of wind energy systems", Wiley-IEEE, pp. 55-58, 2011

[13] S. Z. Chen, N. C. Cheung, K. C. Wong, J. Wu, "Grid synchronization of doubly-fed induction generator using integral variable structure control," IEEE Transactions on Energy Conversion, vol. 24, no. 4, pp. 875-883, 2009. doi:10.1109/TEC.2009.2025316

[14] S. Z. Chen, N. C. Cheung, Y. Zhang, X. M. Tang, "Improved grid synchronization control of doubly fed induction generator using unbalanced grid voltage," IEEE Transactions on Energy Conversion, vol. 26, no. 3, pp. 799-810, 2011. doi: 10.1109/TEC.2011.2158580

[15] A. G. Abo-Khalil, "Synchronization of DFIG output voltage to utility grid in wind power system," Renewable Energy, vol. 44, pp. 193-198, 2011. doi:10.1016/j.renene.2012.01.009

[16] R. Pena, J. C. Clare, G. M. Asher, "Doubly fed induction generator using back-to-back PWM converters and its application to variable speed wind-energy generation," in IEE Proceedings-Electric Power Applications, vol. 143, no. 3, pp. 231-241, 1996. doi:10.1049/ip-epa:19960288

[17] N. Jaalam, N. A. Rahim, A. H. A. Bakar, C. Tan, A. M. A. Haidar, "A comprehensive review of synchronization methods for grid-connected converters of renewable energy source," Renewable and Sustainable Energy Reviews, vol. 59, pp. 1471-1481, 2016. doi:10.1016/j.rser.2016.01.066

[18] W. Sadara, B. Neammanee, "Implementation of a three phase grid synchronization for doubly-fed induction generators in wind energy system," ECTI-CON2010, Chiang Mai, 2010, pp. 1-5.

[19] L. Xiong, P. Li, F. Wu, M. Ma. M. W. Khan, J. Wang, "A coordinated high-order sliding mode control of DFIG wind turbine for power optimization and grid synchronization," International Journal of Electrical Power & Energy Systems, vol. 105, pp. 679-689, 2019. doi:10.1016/j.ijepes.2018.09.008

[20] M. A. S. Ali, K. K. Mehmood, S. Baloch, C. H. Kim, "Modified rotor-side converter control design for improving the LVRT capability of a DFIG-based WECS," Electric Power Systems Research, vol. 186, 2020. doi:10.1016/j.epsr.2020.106403

[21] IEEE application guide for IEEE Std 1547™, IEEE standard for interconnecting distributed resources with electric power systems, IEEE Std 1547.2™-2008